

RAPIDLY VARIED UNSTEADY FLOW IN A SMALL-SCALE DRY BED MODEL

Y. Hassanzadeh

*Faculty of Engineering
University of Tabriz
Tabriz, Iran*

Abstract In this paper the rapidly varied unsteady flow caused by the failure of a dam in a rectangular dry bed horizontal channel has been studied both theoretically and experimentally. Experiments with dam-break flows in smooth and rough channel have been carried out. Comparisons have been made between measured depth hydrographs at different stations along the channel and analytical solution of Ritter and Dressler in this respect. It is concluded that the forward zone of flow is highly sensitive to hydraulic resistance, consequently the measured forward wave velocities are markedly lower than those of theoretical one given by Ritter's solution. The roughness elements in the model, simulating the forest trees in prototype valley at downstream of the dam, tend to decrease the flow velocities and to increase flow depths. Finally the comparison showed that the experimental data of rough channel agreed closely with Dressler's solution. Thus, this latest theory may provide more satisfactory results for hydraulic prototype provisions.

Key Words Dam-Break Problem, Dam Failure, Dam-Break Flood, Rapidly Varied Unsteady Flow

چکیده در این مقاله جریان متغییر سریع غیر دائمی ناشی از شکست سد در یک کانال مستطیلی افقی بدو خشک، از نقطه نظر تئوری و تجربی مورد بررسی قرار گرفته است. آزمایشات توسط جریان حاصل از شکست سد در کانال صاف و زبر انجام پذیرفته است. داده های تجربی اندازه گیری شده از ارتفاع های هیدروگراف ها در ایستگاههای مختلف در طول مسیر جریان، با راه حل تحلیلی ریتز و درسلر مورد مقایسه قرار گرفته است. نتایج حاصله نشان می دهد که ناحیه پیشانی موج نسبت به مقاومت در مقابل جریان بسیار حساس بوده و در نتیجه سرعت های واقعی پیشانی موج بطور محسوسی از مقادیر تئوری ریتز کمتر می باشد. وجود عناصر زبر در مدل که وجود درختان جنگلی را در دره پایاب سدها تشابه سازی می نماید، موجب کاهش سرعت و افزایش عمق جریان می گردد. بالاخره از مقایسه و ارزیابی داده ها چنین استنباط می شود که داده های تجربی کانال زبر با تئوری درسلر همخوانی خوبی داشته و در نتیجه برای محاسبات هیدرولیکی پروتوتیپ ها، تئوری اخیر نتایج رضایت بخشی خواهد داشت.

INTRODUCTION

The flood caused by the rupture of a dam is basically different from natural floods for the following reasons:

- 1- Attenuation of very high peak discharge values in a very short period of time,
- 2- Achievement of important dynamic effects,
- 3- Transport of considerable solid materials, and
- 4- Shock waves occurrences.

Therefore, to prepare a flood map with maximum water levels and the flood front arrivals for each

prototype is necessary. One of the aims of hydraulic engineering is to try to predict these occurrences.

A large number of dam failures are caused by sudden or unpredictable events such as adverse hydrological conditions, gate malfunctioning and foundation or seismic effects. Most of the damages caused by the failure of a large dam are due to the flood resulting from the sudden emptying of the reservoirs. So, it is highly recommended to develop flood emergency plans including inundation maps and evacuation plans, and to provide knowledge of flood propagation and downstream zoning before the occurrence of such a

catastrophic event. Dam break problem has a great practical importance, not only for the applications involving dynamiting of dams through military actions, for example the destruction in 1941 by Russian engineers of the Dnieprostroy Dam (43m height), near Kikass on the Dnieper river, and likewise the bombardment of Mohne Dam (45m height) on Eder river in 1943 [1], but also for occasional mechanical failures of the dams. Some of the most notable dam failures in the past several years include the Buffalo Creek Dam in West Virginia; the Teton Dam near Newdale, Idaho; Laurel Run Reservoir Johnstown in Pennsylvania; and Malpasset Dam in France [2]. Occurrences of a series of dam failures and the associated damage have highlighted the importance of modeling dam-break flows for designing analytical solution to dam-break flows by Ritter [3], this problem has been examined continuously by researchers. The one-dimensional, or x-t representation of dam break has received a wide variety of treatments. These range from the graphical characteristics method of Craya [4] and analytical solution of Dressler [6]; to the numerical models of Sakkas and Strelkoff [7]; Fennema and Chaudhry [8]; and more recently Hou, Hassanzadeh, Nguyen and Kahawita [9].

In the present study, it is shown that the measured velocities for forward wave were as low as 43-56 percent of the theoretical one given by Ritter, on the one hand and the presence of roughness elements in model, simulating the forest trees in prototype, tends to increase the flow depth and retards the flow velocity, on the other hand. It is also, understood that an increase in the time, increases the flow depth along the channel.

CHARACTERISTIC FORMS OF EQUATIONS

By assuming

- hydrostatic pressure distribution,

- horizontal stream bed in a rectangular channel with initially no water below the dam and water at rest above the dam,
- uniform velocity distribution in the vertical direction,

The governing Saint-Venant equations in terms of two dependent variables, mean velocity of flow V and water depth h , and two independent variables, distance x measured downstream along the channel bed (Figure 1) and time t are given as follows:

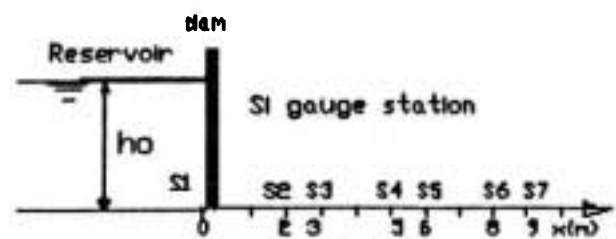


Figure 1. Dam-break model in a dry-bed channel

- continuity equation

$$h \frac{\partial V}{\partial x} + V \frac{\partial h}{\partial x} + \frac{\partial h}{\partial t} = 0 \quad (1)$$

- dynamic equation

$$V \frac{\partial V}{\partial x} + g \frac{\partial h}{\partial x} + \frac{\partial V}{\partial t} = -gJ \quad (2)$$

with $J = V^2 n^2 / R_H^{4/3}$

Where J = energy grade line slope, g = gravitational acceleration and n = Manning roughness coefficient. The characteristics method converts the equations into four total differential equations as follows: For C^+ families characteristic lines:

$$(V+c) \frac{\partial(V+2c)}{\partial x} + \frac{\partial(V+2c)}{\partial t} = \frac{d(V+2c)}{dt} = -gJ \quad (3)$$

$$\frac{dx}{dt} = V+c \quad (4)$$

For C^- families characteristic lines:

$$(V - c) \frac{\partial (V-2c)}{\partial x} + \frac{\partial (V-2c)}{\partial t} = \frac{d(V-2c)}{dt} = -gJ \quad (5)$$

$$\frac{dx}{dt} = V - c \quad (6)$$

Where $c = \sqrt{gh}$ represents the celerity of a small gravity wave. The first C^+ and C^- Equations of 3 and 5 are valid only when the second Equations of 4 and 6 in each group are satisfied. The total derivative operators represent the rate of change from the viewpoint of imaginary observers moving with velocities $(V+c)$ and $(V-c)$ respectively. It means that the paths of these two imaginary observers can be traced on the independent variable plane, i.e., the $x-t$ plane shown in Figure 2, and a complete solution may be obtained for any prescribed unsteady flow situation. For the simplest cases the process leads to analytical solution, but in the more complex cases numerical solutions of the governing partial differential equations, finite-difference or finite-element methods may be used.

By ignoring the effects of the frictional and turbulence resistance to unsteady flow and by setting $J=0$, the characteristics equations may

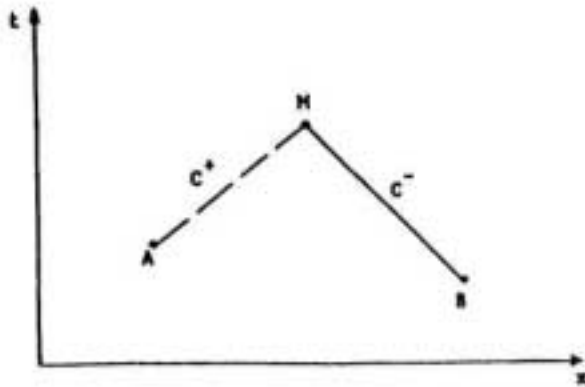


Figure 2. Tex x-t plane

be reduced as follows:

$$\frac{d(V \pm 2c)}{dt} = 0 \quad (7)$$

$$\frac{dx}{dt} = V \pm c \quad (8)$$

Where the velocities are considered positive in the downstream direction and negative in the upstream direction.

Sudden destruction of a dam results in a highly unsteady flow, with a forward wave (positive wave) advancing over a dry channel with the constant speed of $2c_0 = 2\sqrt{gh_0}$, and a back disturbance (negative wave) propagating into the still water above the dam with the speed of $c_0 = \sqrt{gh_0}$. In the disturbed region between these two extremes, the particle velocity V , the celerity of gravity wave c and the flow depth h should be determined. It is clear that in the $x-t$ plane the slope of C^- and C^+ characteristic lines represent $V-c$ and $V+c$, respectively and along the C^- and C^+ characteristics the quantity $V-2c$ and $V+2c$ are respectively constant. It follows that along the C^+ characteristic lines in the disturbed zone, we would have:

$$V+2c = 2c_0 \quad (9)$$

Since $V_0 = 0$

And along the negative characteristics lines C^- in this zone the relation may be indicated as:

$$\frac{dx}{dt} = \frac{x}{t} = V-c = 2c_0 - 3c = \frac{3}{2} V-c_0 \quad (10)$$

From which we could obtain the following relations in dimensionless form to determine the variable quantities:

$$V^* = \frac{V}{c_0} = \frac{2}{3} \left(1 + \frac{x}{tc_0}\right) \quad (11)$$

$$c^* = \frac{c}{c_0} = \frac{1}{3} \left(2 - \frac{x}{tc_0}\right) \quad (12)$$

$$h^* = \frac{h}{h_0} = \frac{1}{9} \left(2 - \frac{x}{tc_0}\right)^2 \quad (13)$$

$$q^* = \frac{q}{c_0 h_0} = \frac{8}{27} - \frac{2}{9} \left(\frac{x}{tc_0}\right)^2 + \frac{2}{27} \left(\frac{x}{tc_0}\right)^3 \quad (14)$$

Where q^* represents the discharge per unit width of channel in dimensionless form. Eliminating x/tc_0 from Equations 11 and 12, shows that V^* and c^* obey the following relation along the negative characteristic lines.

$$V^* = 2(1 - c^*) \quad (15)$$

The above analytical solution of dam break problem was given first by Ritter [3], from which we get the results that for reasons of continuity, the depth, velocity and discharge rate at dam site will have the constant magnitudes, and the flow should take place at critical state, $V^* = c^* = \frac{2}{3}$; $h^* = \frac{4}{9}$; $q^* = \frac{8}{27}$. The dimensionless presentation of Ritter solution is shown in Figure 3 and Figure 4. The inspection of the characteristics Equation 8 and Figure 4 indicates that both families of characteristics (C^+ and C^-) coincide along the forward front wave, where $c^* = 0$ and the velocity of forward front wave becomes identical with the fluid velocity $V^* = 2$. In Figure 4 the solid lines are the characteristics obtained by using the minus sign and the dashed curves are the characteristics obtained by using the plus sign in Equation 8.

By using the perturbation method, considering the hydraulic resistance effect ($J > 0$) and ignoring the bed slope of channel, Dressler [6] obtained the following relations to calculate the variables quantities in dimensionless form:

$$V^* = \frac{2}{3} (1+m) + 1(m) RT \quad (16)$$

$$c^* = \frac{1}{3} (2-m) + k(m) RT \quad (17)$$

With

$$1(m) = -\frac{108}{7} \frac{1}{(2-m)^2} + \frac{12}{2-m} - \frac{8}{3} + \frac{8\sqrt{3}}{189} (2-m)^{3/2} \quad (18)$$

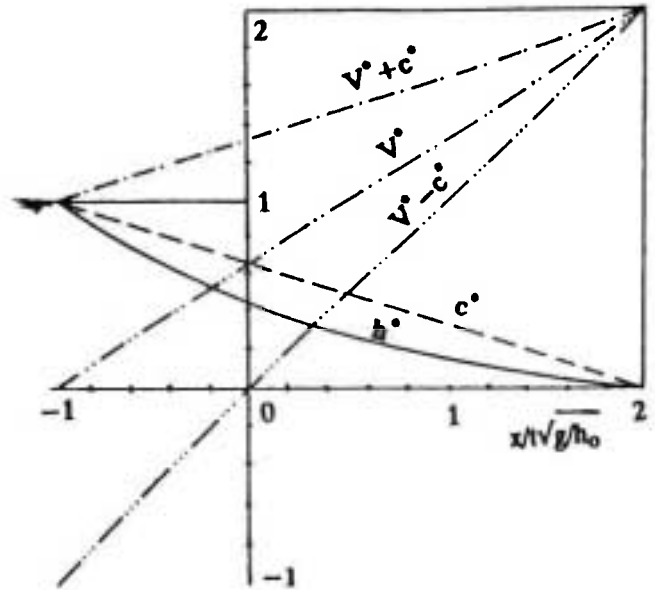


Figure 3. Variation of Dimensionless Values in terms of $x/t \sqrt{g/h_0}$

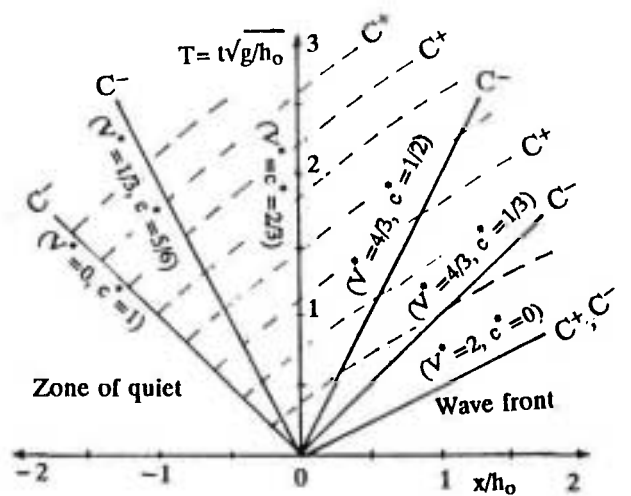


Figure 4. The dimensionless presentation of Ritter solution

$$k(m) = \frac{6}{5(2-m)} - \frac{2}{3} + \frac{4\sqrt{3}}{135}(2-m)^{3/2} \quad (19)$$

$$m = \frac{x}{t c_0} = \frac{x/h_0}{t \sqrt{g/h_0}}; T = t \sqrt{g/h_0}; R = n^2 \cdot g / R_H^{1/3} \quad (20)$$

EXPERIMENTAL FACILITY

Positive waves in the channel and negative waves in the upstream reservoir were generated by a dam-break mechanism which suddenly removed a plate separating the reservoir from the channel. The channel had a rectangular cross section of 0.91m width, and 1.05m height with a usable length of about 24m. It was equipped with a recirculating water supply system, including a storage tank, and a pump. The dam-break mechanism consisted for a wooden gate of 1.2m height and 0.91m length which was pivoted at its upper edge, so that it was rotated about a horizontal axis. The gate simulating the dam was placed mid-length along the channel and the time of its opening was about 0.1 second. The dam was then removed instantaneously. The upstream reservoir had a constant depth of $h_0 = 0.30\text{m}$. The measurements of depth and wave front celerity were made with a churchill control, model 1858-07900. The wave monitor was equipped with a 7 channel system. The depth variation with time was recorded using 7 depth gauges which were situated at downstream distances of $x = 0, 2, 3, 5, 6, 8, 9\text{m}$ along the channel from the dam (Figure 1).

The channel had a painted steel bottom and plate glass sides. Tests were conducted using a nearly smooth and a rough channel bottom. The nearly smooth channel bottom was determined in metric unit with Dressler's formula to have a Manning coefficient, n , of about 0.016. The roughness elements in the rough channel of the downstream of the dam, simulating the forest trees, consisted of two series of cubic of wood blocks fastened to the floor at

6 cm intervals (center line distance). The dimensions of wood blocks in the first series were $1\text{cm} \times 1\text{cm} \times 1\text{cm}$, and in the second one they were $1\text{cm} \times 1\text{cm} \times 2\text{cm}$. It means that the height of the roughness elements in the first and second series were 1cm and 2cm respectively, perpendicular to the channel bottom and the cross-section of these elements was constant, i.e. 1cm by 1cm. The roughness elements in the model, simulating the forest trees in prototype, were fixed on the bottom channel, so, these elements were not free to move under the influence of the hydrodynamic forces exerted by the flow. The Manning roughness coefficient, n , were determined in metric unit with Dressler's formula to be $n = 0.018$ and $n = 0.02$.

ANALYSIS AND RESULTS

Three sets of experiments on dam-break flows in nearly smooth ($n = 0.016$) and rough channel ($n = 0.018, n = 0.02$) are made in constant hydraulic conditions (i.e., reservoir depth $h_0 = 0.30\text{m}$, and dry bed channel). The variation of flow depth with time in the channel at six stations ($x = 2, 3, 5, 6, 8, 9\text{m}$), and the variation of water level with time at dam-site ($x = 0$) were recorded during each test. The celerities of wave front in both smooth and rough channel were calculated and compared (Table 1) with the theoretical result given by Ritter's solutions $c_f = 2c_0$. As indicated in Table 1, the measured celerities for forward wave were as low as 43 percent for the smooth channel and 56 percent for the rough channel.

The variation of depth hydrographs with the distance x/h_0 and time T are presented in Figure 5. It is observed that for a given Manning coefficient, with increased time, on one hand the flow depth increases, and for a given time as well as a given Manning coefficient, by increasing the distance, the flow depth decreases, on the other hand. Also, comparing the experimental data, for smooth and rough channel,

TABLE 1. Celerities of Wave Fronts, C_p (m/s)

Station Nr. \ n	1 to 2	2 to 3	3 to 4	4 to 5	5 to 6	6 to 7	2 to 7	$\frac{2C_0 - C_{f2-7}}{2C_0}$
0.016	2.29	1.97	1.84	1.83	1.89	1.96	1.97	43%
0.018	2.12	1.46	1.65	1.68	1.58	1.50	1.58	54%
0.02	1.97	1.45	1.62	1.49	1.49	1.45	1.52	56%

through the analytical solution showed that for $5 \leq T \leq 30$, there was a good agreement between experimental data and Ritter solution.

For nearly smooth channel, ranging $30 < T < 60$, the

Ritter solution confirmed satisfactorily by the experimental data, whilst, for rough channel, and $T > 60$ the Dressler solution could be confirmed by the experimental data. Notable is that, our results [10] were in a good accordance with those of some other researchers [11,12,13,14], obtained for the model and prototype studies.

Comparisons between measured depth hydrographs and analytical solution of the problem for both smooth and rough channel have been made in Figure 6. Thereafter, the nearly smooth channel data agreed closely with the Ritter solution for the downstream channel ($x/h_0 = 10, 20, 30$), while, there was a good agreement between the rough channel data and Dressler solution. It must be noted that, at the dam site ($x/h_0 = 0$), and for $5 < T < 30$, the experimental data agreed closely with the analytical solution of the problem, but in the range of $5 < T \leq 0$ and $T > 30$, there were some divergences between observed data and analytical solution.

The dimensionless flow rate hydrographs, for different values of n , are presented in Figure 7. It could be observed that, with increasing the time, the flow rate increases, and through the increased roughness coefficient, the flow rate decreases.

The variation of Froude number, F_r , with respect of time, T , and roughness coefficient, n , has been calculated and presented in Figure 8. It is revealed that at a given station, x/h_0 , and for a given roughness coefficient, n , increasing the time, T , the Froude number, F_r , decreases. Also, at a given station and for a given time, the Froude number decreases by an increase in the roughness coefficient. In the present

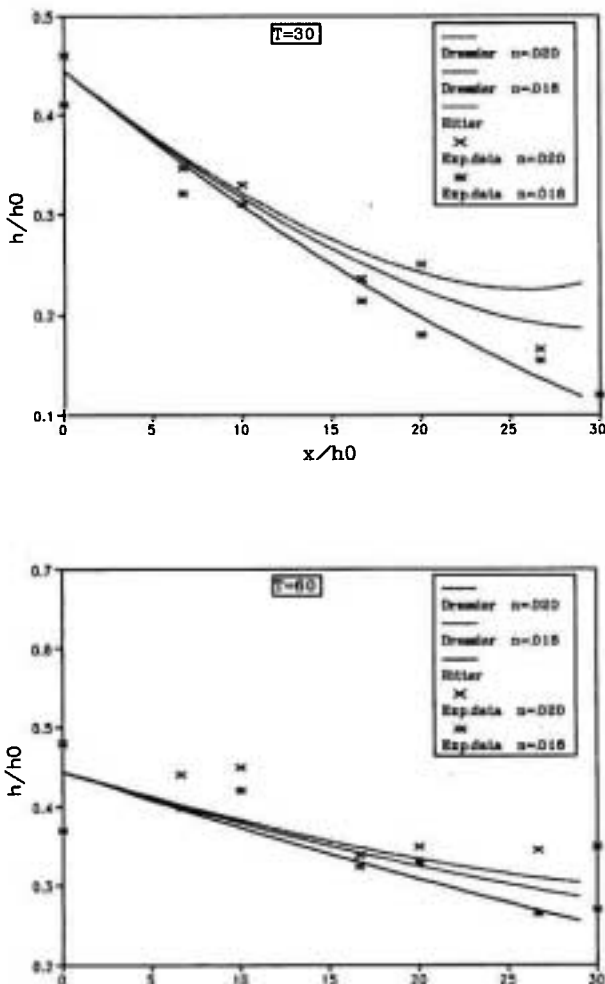


Figure 5. Variation of h/h_0 with x/h_0 for different values of n .

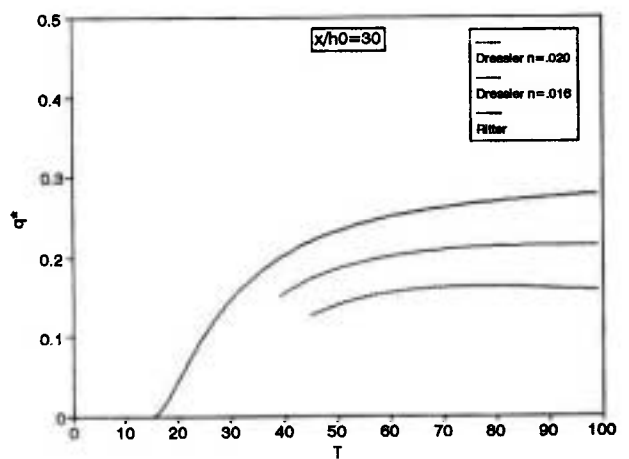
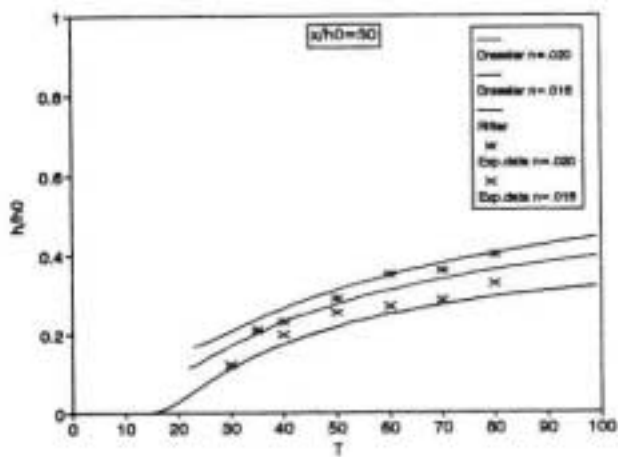
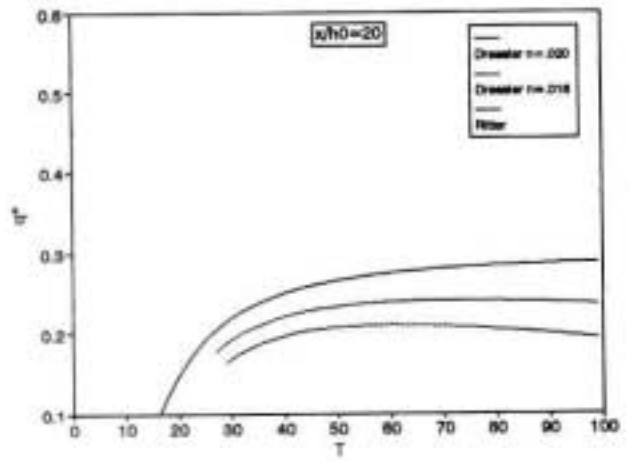
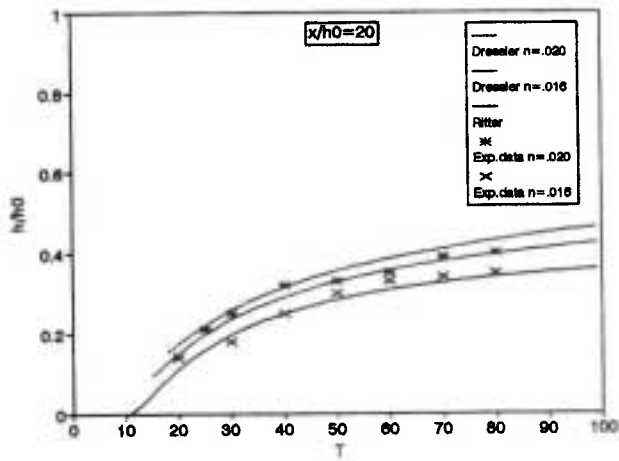
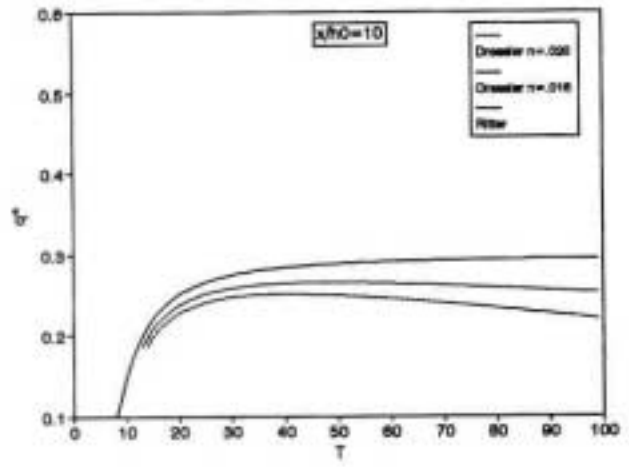
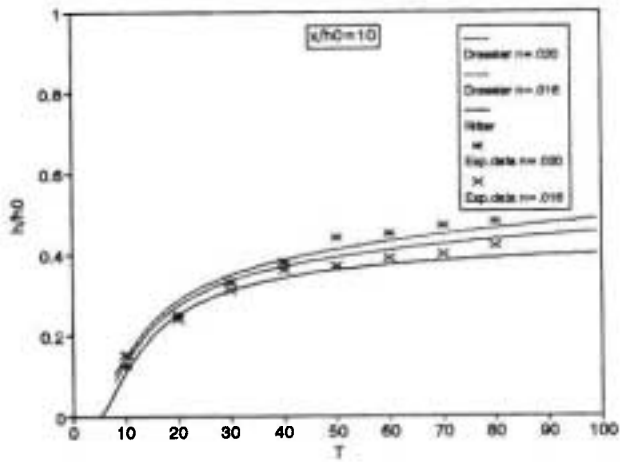


Figure 6. Variation of h/h_0 with T for different values of n .

Figure 7. Dimensionless flow rate hydrographs, for different values of n .

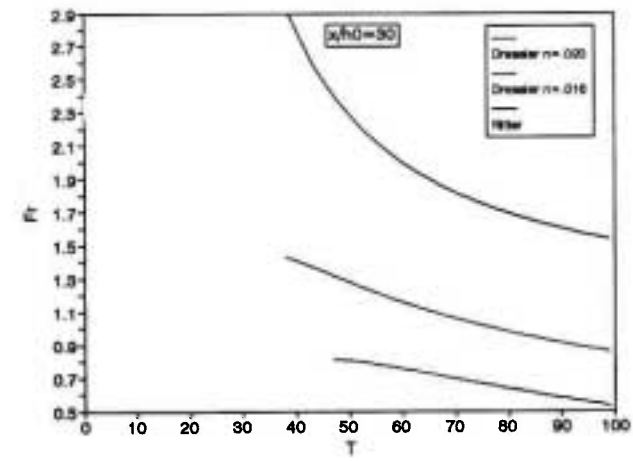
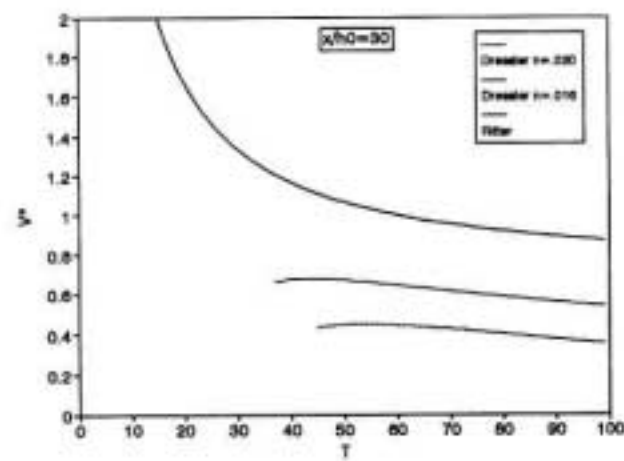
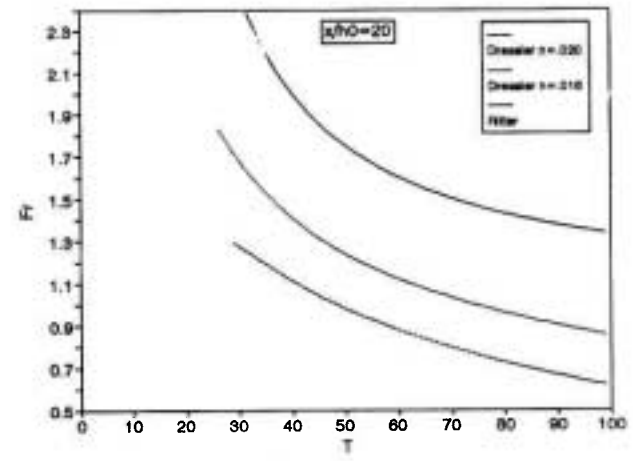
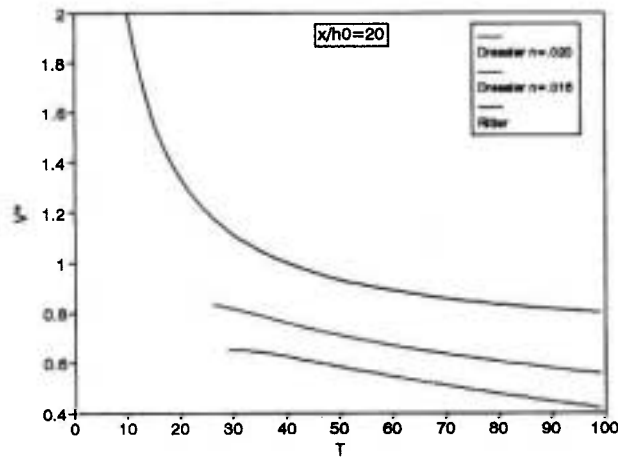
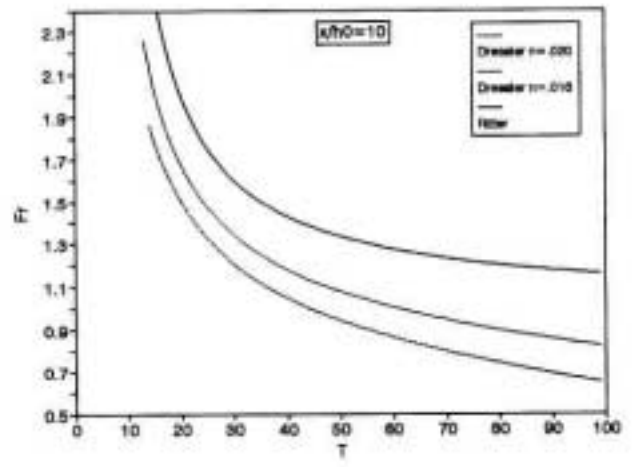
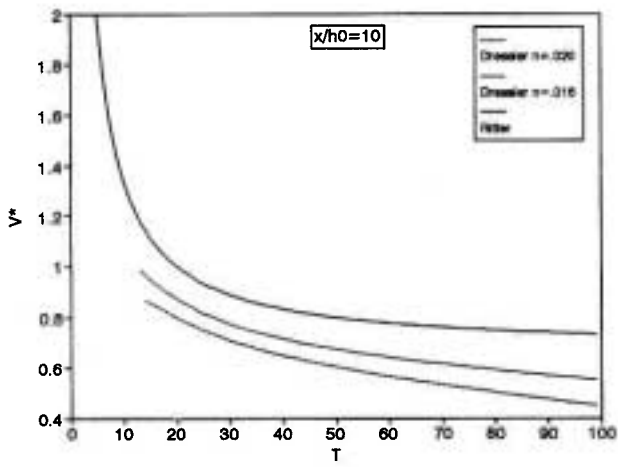


Figure 8. Variation of Fr with T for different values of n .

Figure 9. Variation of V^* with T for different values of n .

study, once the time increased from 10 to 80, the Froude number decreased from about 2.7 (supercritical flow) to 0.9 (subcritical flow), for $n=0.016$, and from about 2.4 to 0.73 for $n=0.02$. It is obvious that, through an increase in the roughness coefficient, the time of critical occurrence conditions decreases (i.e., at $x/h_0 = 10$, for $n=0.016$, and $n=0.02$, the critical occurrence conditions reached up to $T=60$ and $T=44$ respectively).

The variation of flow velocities, V^* , with time, T , for different values of n , are presented in Figure 9. It is seen that, in a given station, by increasing the time and Manning coefficient, there would be decreases in the velocities along the channel.

CONCLUSIONS AND DISCUSSIONS

The conclusions drawn from this investigation were as follows:

- I- The obtained data showed that the measured velocities for the forward wave were as low as 43-56 percent of the theoretical one given by Ritter without resistance, whereas the experimental and theoretical results agreed closely with the tip of the negative wave. In other words, the forward zone of the flow was highly sensitive to hydraulic resistance. It should be noted that the loss of energy in dam-break turbulent flow over a rough surface is due largely to the formation of waves behind each roughness element.
- II- The presence of roughness elements on bottom channel tends markedly to increase flow depth and retards the flow. Thus, the roughness in terms of Manning's n can be taken as dominating factor that affects the flow depth and velocity.
- III- The experiments indicated that with increasing the time the flow depth along the channel increases as well.
- IV- The comparison of theoretical and experimental data showed that the Dressler solution gives more

satisfactory results than the Ritter's solution.

- V- Our learnings through conducting the investigation, would help us to well develop our knowledge on flood propagation and its consequences. Also, it would be greatly recommended to prepare flood emergency plans including flood damage reduction projects, floodplain management programs, inundation maps with maximum water levels and the flood front arrivals for each prototype.

NOMENCLATURE

c	celerity
h	flow depth
h_0	reservoir depth
R_H	Hydraulic radius
n	Manning rouffness coefficient
J	energy grade line slope
g	gravitational acceleration
V	flow velocity
x	distance along the channel
t	time
T	dimensionless time
q	discharge per unit width
*	indicates the dimensionless values

REFERENCES

1. R. H., Honoré "Un Aspect de la Guerre Moderne, les Briseure de Barrage", La Houille Blanche, (1945), 69-74.
2. A. Goubet, "Risques Associés aux Barrages", La Houille Blanche, No. 8, (1979).
3. A. Ritter, "Die Fortpflanzung der Wasserwellen". Zeitschrift des Vereines Deutscher Ingenieure", Vol. 36, No. 3 (1892), 974-954.
4. A. Craya, "Calcul Graphique Des Regimes Variables Dans Les Canaux." La Houille Blanche, No. 1, 19-38 and No. 2, (1946), 117-130.
5. R. Ré, "Etude du Lacher Instantané D'une Retenue

- Dans Un Canal Par La Méthode Graphique". *La Houille Blanche*, (1946).
6. R.F. Dressler, "Hydraulic Resistance Effect upon the Dam-Break Functions" *Journal of Research of the National Bureau of Standard*, Vol. 49, No 3, (1952), 217-225.
 7. J. G. Sakkas and T. Strelkoff, "Dimensionless Solution of Dam-Break Flood Waves". *Journal of Hydraulic Division, A.S.C.E.*, 102 (HY2), (1976) 171-184.
 8. R. J. Fennema and M. H. Chaudhry, "Implicit Methods for two-Dimensional Unsteady Free-Surface Flows", *Journal of Hydraulic Research.*, Vol. 27. No 3, (1984), 321-332.
 9. Z. Hou, Y. Hassanzadeh, D. L. Nguyen, R. Kahawita, "A 1-D Numerical Model Applied to Dam-Break Flows on Dry-Beds". *Journal of Hydraulic Research*, Vol. 30, No 2. (1992) 211-224.
 10. Y. Hassanzadeh, "Rapidly Varied Unsteady Flow Study in a Small-Scale Model" *Proceeding of the International Conference on Hydrodynamics, Wuxi, China (1994)*, 596-603.
 11. C. Marche, G. Lessard, S., et Lemaire, "Rupture de Barrage et Cartographie des Inondation, une Analyse Assistée par Ordinateur" *CAN. J. CIV. ENG.* Vol. 17, CANADA (1990).
 12. L. Escande, J. Nougaro, L. Castex and H. Barthet, "Influence de Quelques Paramètres sur une onde de Crue Subite à l'aval d'un Barrage" *La Houille Blanche*, No 5 France (1961).
 13. M. Gallanti and L. Ubertini, "Hydrological Problems of Dam and Levee Rupture" *Proceedings of the Technical Conference in Geneva*", World Meteorological Organization (Nov. 1988) 178-191.
 14. D. L. Fread, "National Weather Service Models to Forecast Dam-Breach Floods" *Proceedings of the Technical Conference in Geneva*, (Nov. 1988), World Meteorological Organization 192-211.